RESEARCH ARTICLE

Elucidation of artefacts in proton transfer reaction time-of-flight mass spectrometers

Jorge Iván Salazar Gómez[1] (ID) | Christian Klucken[1] | Martha Sojka[1] | Liudmyla Masliuk[2] | Thomas Lunkenbein[2] | Robert Schlögl[1,2] | Holger Ruland[1]

[1] Department of Heterogeneous Reactions, Max Planck Institute for Chemical Energy Conversion, Mülheim a.d. Ruhr, Germany

[2] Department of Inorganic Chemistry, Fritz Haber Institute of the Max Planck Society, Berlin, Germany

Correspondence
Jorge Iván Salazar Gómez and Holger Ruland, Department of Heterogeneous Reactions, Max Planck Institute for Chemical Energy Conversion, Stiftstrasse 34-36, Mülheim a.d. Ruhr 45470, Germany.
Email: jorge-ivan.salazar-gomez@cec.mpg.de; holger.ruland@cec.mpg.de

Funding information
Federal Ministry of Education and Research, Grant/Award Numbers: 03EK3037C and 03EK3546

Abstract

We present an effective procedure to differentiate instrumental artefacts, such as parasitic ions, memory effects, and real trace impurities contained in inert gases. Three different proton transfer reaction mass spectrometers were used in order to identify instrument-specific parasitic ions. The methodology reveals new nitrogen- and metal-containing ions that up to date have not been reported. The parasitic ion signal was dominated by $[N_2]H^+$ and $[NH_3]H^+$ rather than by the common ions NO^+ and O_2^+. Under dry conditions in a proton transfer reaction quadrupole interface time-of-flight mass spectrometer (PTR-QiTOF), the ion abundances of $[N_2]H^+$ were elevated compared with the signals in the presence of humidity. In contrast, the $[NH_3]H^+$ ion did not show a clear humidity dependency. On the other hand, two PTR-TOF1000 instruments showed no significant contribution of the $[N_2]H^+$ ion, which supports the idea of $[N_2]H^+$ formation in the quadrupole interface of the PTR-QiTOF. Many new nitrogen-containing ions were identified, and three different reaction sequences showing a similar reaction mechanism were established. Additionally, several metal-containing ions, their oxides, and hydroxides were formed in the three PTR instruments. However, their relative ion abundancies were below 0.03% in all cases. Within the series of metal-containing ions, the highest contribution under dry conditions was assigned to the $[Fe(OH)_2]H^+$ ion. Only in one PTR-TOF1000 the Fe^+ ion appeared as dominant species compared with the $[Fe(OH)_2]H^+$ ion. The present analysis and the resulting database can be used as a tool for the elucidation of artefacts in mass spectra and, especially in cases, where dilution with inert gases play a significant role, preventing misinterpretations.

KEYWORDS

artefacts, industrial gases, parasitic ions, proton transfer reaction time-of-flight mass spectrometry, volatile organic compounds

1 | INTRODUCTION

In the last decades, chemical ionization mass spectrometry (CIMS)[1,2] was established as a new and powerful tool for the on-line monitoring of trace amounts of volatile organic compounds (VOCs) without requiring additional pre-separation techniques such as gas chromatography. One of the important improvements of CIMS was the use of the hydronium (H_3O^+) cation as primary ionization ion, which has led

to the development of proton transfer reaction mass spectrometry (PTR-MS).[3] Originally, this technique was applied to determine VOCs in air.[4] Nowadays, PTR-MS has a broad application in different fields, which ranges from food science[5-7] over life[8,9] and environmental science[9-12] to process monitoring.[13-16] However, reports on industrial or catalytic applications are scarce.[17-19] One of the main advantages of PTR-MS is the rather "soft" ionization of molecules by the primary ion H_3O^+, such that the proton transfer can be considered to be almost nondissociative but there are some exceptions (alcohols[20] and terpenes[21]). Because of the low fragmentation, this technique allows the detection of molecules at their molecular mass plus one H^+, and thus, it enables the analysis of complex gas mixtures without the need for previous separation methods. However, the identification of isomeric compounds becomes difficult since they have the same nominal mass for the protonated molecule. If the mass resolution is above 4000 $m/\Delta m$, some isobaric compounds can be identified.[22] To further enhance the selectivity towards the separation of isobaric ions, the coupling of a time-of-flight (TOF) mass analyser to a PTR ion source was demonstrated.[23] The advantages of TOF over quadrupole mass filters are their higher mass resolution, their short response time (1 s or less), the simultaneous measurement of the whole mass spectrum, and a virtually unlimited mass range.

Analyte gases must have a larger proton affinity than water (691 kJ mol^{-1}) in order to enable the proton transfer:

$$R + H_3O^+ \rightarrow [R]H^+ + H_2O, \tag{1}$$
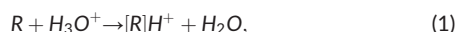
where R is a gas phase analyte. This reaction is exothermic and proceeds at reaction rates that are close to the rate of collision (approximately: 10^{-9} cm^3 molecule^{-1} s^{-1}).

In addition, the main components of air, such as nitrogen, oxygen, carbon dioxide, and methane, exhibit lower proton affinities than water and thus are not measurable. This means VOCs in these gases can be analysed without dilution, which enhances the detection limit of the VOCs. The main drawback of PTR is the presence of parasitic ions, such as NO^+, O_2^+, water clusters $[(H_2O)_n]H_3O^+$, $[NH_3]H^+$, and $[N_2]H^+$. The presence of small amounts of NO^+ and O_2^+ has been ascribed to back diffusion of air from the drift tube region.[24] In order to minimize unwanted reactions, the amount of these ions should be less than 2% of the total ion intensity.[25,26] Ideally, i.e., in the absence of back diffusion, only water vapour would be present in the ion source, and after electron impact, the H^+, O^+, H_2^+, OH^+, and H_2O^+ ions are formed. Subsequently, these ions can react with water molecules in the "source drift region" and produce H_3O^+ ions with a purity of about 99.5%.[4]

As opposed to the typical environmental application of PTR[27,28] in which humidity and gas matrix composition are kept almost constant, in catalytic processes, the gas matrix can change from dry to humid (eg, methanol synthesis[29]). Moreover, in standard applications, the analytes are already diluted in the air sample. Thus, no additional dilution is needed, as typical concentrations already are in the desired ppb range. Sometimes, it is even necessary to pre-concentrate the gas samples[30] in order to increase the sensitivity of the method.[31] In the analysis of industrial gases, however, dilution is required in order to

avoid pressure changes in the detection region of the instrument as well as remain in the linearity range of the detector.[17] In particular, avoiding the saturation of the detector is challenging since the concentration range of many compounds of interest may be quite different. Consequently, the concentration of analytes that are already present in the ppb-range can fall below the detection limit of the instrument because of dilution, making their identification and quantification challenging.

In this work, we focus on the PTR-TOF-MS analyses of measurements that were carried out using nitrogen 5.0 (99.999% purity) and nitrogen 6.0 (99.9999%) from two different suppliers on three different PTR instruments to unravel the origin of possible artefacts in the mass spectrum. In order to identify impurities in the nitrogen gas 5.0, which may also be present as memory effects, a comparison was carried out with a gas of higher purity (N_2 6.0) with and without further purification through a filter. A memory effect can be the result of a short-time high-concentration peak for a sticky substance that is adsorbed on inlet lines or instrument parts and slowly desorbs, thus, being present in the spectra for long time. However, if certain adsorbing sites (eg, O-rings and septa) are available, some substance can be enriched and then gradually desorbed. For the characterization of trace compounds in complex gas matrices, such as industrial gases (before and after purification) or the products of some catalytic reactions, it is crucial to understand the contribution of artefacts to the mass spectrum, especially in cases where dilution with inert gases, such as nitrogen, is compulsory. These artefacts may originate from the instrument and can coincide with some substances of interest or can even cause side reactions. In addition, we show that some parasitic ions exhibit a humidity dependence. This implies that the typical background subtraction procedure is only suitable if the gas sample and the background have the same humidity level. Otherwise, wrong estimations and misinterpretations could be made. Comparative measurements with three different instruments located at two different sites may allow for assigning some of the peaks observed in the spectra of pure nitrogen as instrument dependent, memory effect, or gas contaminant. In order to compare the data, all instruments have the same type of ion source, and the experiments were carried out under similar conditions (E/N 131 Td). A E/N range between 120 and 140 Td has been established as a standard value, since it is a good compromise between excessive water cluster formation and product ion fragmentation.[8,24]

2 | EXPERIMENTAL SET-UP

2.1 | PTR-TOF-MS instruments

A detailed description of the kind of PTR-MS instruments used in this study has been given by Lindinger et al.[9] and Sulzer et al.[32] In brief, the three instruments used for the comparison measurements were two PTR-TOF1000 instruments located at the Fritz-Haber Institute in Berlin, Germany and a proton transfer reaction quadrupole interface time-of-flight mass spectrometer (PTR-QiTOF) located in a mobile lab container on a steel mill plant in the Ruhr area in Germany. Further

information to these instruments is given in Table 1. All instruments were acquired from Ionicon Analytik GmbH, Innsbruck, Austria. These instruments possess the same type of ion source, but the PTR-QiTOF (PTR-1) differs in its quadrupole interface, which is connected after the drift tube. This interface serves as an ion guide that focuses the ions and increases the sensitivity.[32] In this study, measurements were conducted using H_3O^+ as primary ion. H_3O^+ ions are generated in the hollow cathode ion source using a water vapour flow of 7 sccm in the PTR-QiTOF and 6.5 sccm in both PTR-TOF1000. The parameters for the drift tube of the PTR-QiTOF were set to 900 V, 3.50 mbar, and 60°C resulting in a E/N of about 131 Td. For the PTR-TOF1000 instruments, the drift tube was adjusted to 600 V, 2.39 mbar, and 80°C, which results in an identical E/N value of 131 Td. The inlet temperatures for the PTR-QiTOF and the PTR-TOF1000 were 100°C and 80°C, respectively. In the detection region, both instruments use an orthogonal acceleration. A mass range from m/z 15 up to 797 was used for all instruments. The collected signals are corrected for the individual instrumental transmissions. Mass calibration was carried out using the masses of the internal standard equipped in the PTR-QiTOF and the newer PTR-TOF1000 instruments (PerMaSCal) and the masses of NO^+ (m/z 29.9974) and the second isotope of H_3O^+ ($H_3^{18}O^+$, m/z 21.0221). For simplicity, in the following, it is referred to the second, third, etc isotopes by using a nomenclature according to their order of abundance, eg, $H_3^{16}O^+$ (H_3O^+(1) or simply H_3O^+) and $H_3^{18}O^+$ (H_3O^+(2)). In the case of the PTR-QiTOF prior to the measurements, an optimization of the transmission was carried out with the Thuner Software (TofWerk, Thun, Switzerland). Optimization of the mass of the parasitic ion $[N_2]H^+$ (m/z 29.0134) was conducted in order to minimize its intensity. The masses of protonated toluene (m/z 93.0699) and the two known masses from the internal standard PerMaSCal (m/z 203.9431) and (m/z 330.8475) were set in order to maximize their sensitivities.

The experiments with the PTR-QiTOF were carried out with N_2 5.0 and N_2 6.0 from supplier A. All the measured gases are connected to a Sulfinert-coated flow-through 10-multiport valve (MPV) from VICI Valco. The dry and humidified gases for the background measurements are generated using a certified calibration gas generator (IAS GmbH, Oberursel, Germany), which can generate gas standards of typical VOCs from a few ppb up to hundreds of ppm under dry or humid

conditions. For the nitrogen 6.0, which was additionally purified with a filter, no humidification was possible, since the measurements with this extra purified gas were carried out in order to identify possible artefacts coming from the calibration gas generator and from the filter itself. The filter contains nickel and nickel monoxide as the main constituents and was purchased from the company Rainer Lammertz Pure Gas Products, Huerth, Germany. The heated line (150°C) connecting the calibration gas generator to the MPV has also a Sulfinert coating. The inlet lines of all three PTR-instruments are made of polyether ether ketone (PEEK). Trace analysis on both PTR-TOF1000 instruments were conducted with N_2 5.0 from supplier B. The N_2 gas was directly connected to the respective inlets.

3 | RESULTS AND DISCUSSION

The ion distributions of the primary ion and the water clusters in the three PTR instruments and of the main nitrogen-containing parasitic ions that have been investigated in this work in background measurements are presented in Figure 1 and Table 2, respectively. Less
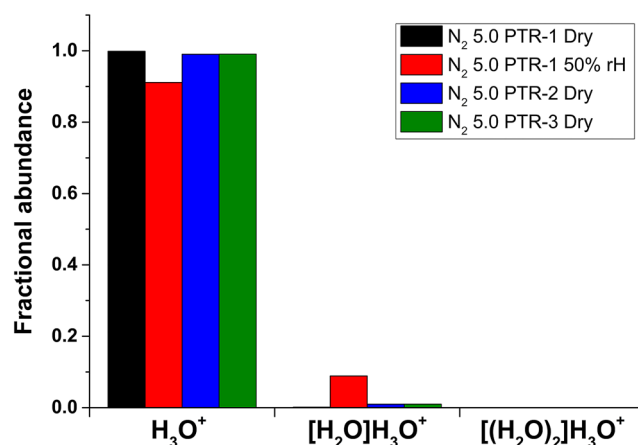

FIGURE 1 Fractional abundance of the primary ion and the first and second water clusters in all three PTR instruments using nitrogen 5.0 under dry and humid conditions (50% rH at 20°C). PTR, proton transfer reaction; rH, relative humidity

TABLE 1 Characteristics of the different PTR-TOF-MS instruments applied in this work

	Instrument		
	PTR-1	PTR-2	PTR-3
Type	PTR-QiTOF	PTR-TOF1000	PTR-TOF1000
Year of commissioning	2015	2015	2018
Location	Lab container at steel mill plant	Fritz-Haber-Institut der Max-Planck-Gesellschaft	Fritz-Haber-Institut der Max-Planck-Gesellschaft
Measurement history[a]	VOCs in air, Coke oven gas, Gas standards	N_2, CO, CO_2, H_2, O_2, Ar, Methanol, Ethylene, Ethane, Propane	N_2
Cleaning of ion source	Twice	—	—

Abbreviations: PTR-QiTOF, proton transfer reaction quadrupole interface time-of-flight mass spectrometer; VOC, volatile organic compound.

[a]Gases contain volatile contaminants.

TABLE 2 Transmission corrected and normalized ion count rates of nitrogen-containing parasitic ions observed under dry and humid conditions in three different PTR-TOF-MS instruments using N_2 5.0 and 6.0

Measured mass at PTR-1 (m/z)	Theoretical mass (m/z)	Chemical formula (tentative assignment)	N_2 5.0 PTR-1		N_2 6.0 PTR-1		N_2 6.0 PTR-1 Filter	N_2 5.0 PTR-2	N_2 5.0 PTR-3
			Dry (ncps)	Humid (ncps)	Dry (ncps)	Humid (ncps)	Dry (ncps)	Dry (ncps)	Dry (ncps)
14.0000	14.0025	N^+	28.40	16.71	28.82	17.36	28.46	574.71	n.d.
15.0085	15.0104	HN^+	16.14	12.05	17.41	11.70	16.52	4.68	1.19
16.0159	16.0182	H_2N^+	336.80	207.64	340.53	213.35	330.74	4.24	2.33
17.0238	17.0260	H_3N^+	2985.92	2456.54	2960.93	2480.08	2963.85	370.33	447.45
18.0319	18.0338	H_4N^+	38960.63	42767.20	37799.85	42327.15	38849.77	8219.00	9633.74
28.0051	28.0068	N_2^+	345.67	62.56	358.38	63.96	346.60	2340.53	11.43
29.0130	29.0134	HN_2^+	n.m.	n.m.	183399.30	26970.92	178195.87	3124.86	1752.89
29.9969	29.9974	NO^+	1324.05	1389.97	1357.42	1438.85	1302.38	1893.97	1789.87
30.0099	30.0105	$HN_2^+(2)$	137611.7	27272.38	144155.73	27853.22	138815.41	106783.6	32305.21
31.0054	31.0053	HNO^+	15.04	5.33	14.27	4.94	13.65	9.09	2.64
31.0284	31.0291	$H_3N_2^+$	9.98	4.52	9.80	4.88	9.39	6.96	0.75
32.0127	32.0131	H_2NO^+	19.92	5.91	23.40	6.10	20.35	75.17	3.52
33.0207	33.0209	H_3NO^+	4.10	3.87	4.08	4.33	4.05	6.36	1.81
34.0286	34.0287	H_4NO^+	16.49	18.83	16.70	18.97	17.05	6.33	1.47
42.0091	42.0087	N_3^+	83.99	42.72	86.71	44.27	81.43	29.26	1.47
44.0171	43.0165	HN_3^+	11.49	14.76	11.41	12.64	10.68	0.00	0.00
44.0011	44.0006	N_2O^+	4.66	1.41	5.18	1.18	4.80	8.04	0.50
44.0248	44.0243	$H_2N_3^+$	4.68	4.55	4.99	4.53	4.78	5.92	0.91
45. 0079	45.0084	HN_2O^+	13.66	5.52	12.69	4.30	12.41	3.81	0.24
49.9936	45.9924	NO_2^+	2.21	5.03	2.11	5.04	2.63	4.80	3.51
56.0130	56.0118	N_4^+	1.40	0.20	1.71	0.22	1.53	15.45	0.40

Abbreviations: n.d., not determined; n.m., not measurable; PTR-TOF-MS, proton transfer reaction time-of-flight mass spectrometry.

dominant artefacts, such as metal-containing ions, are summarized in Table 3. Since in general, the observed artefacts should be independent of the carrier gas used, similar measurements with He and Ar were carried out in comparison. These confirm the presence of the assigned artefact ions in this work in all inert gases commonly used as carrier gas.

3.1 | Main parasitic ions

Among all possible parasitic ions, such as, the well-known NO^+ and O_2^+ or the less reported $[NH_3]H^+$ and $[N_2]H^+$, the water clusters $[H_2O]H_3O^+$ play a significant role in the interpretation of the mass spectra, because of the fact that they can also act as primary ions or cause the formation of association ions, which make more difficult the identification of unknown compounds.

3.1.1 | Water clusters ion distribution

Figure 1 shows the ion distributions of the primary ion and the first and second water cluster ions in all three PTR instruments. The humidified nitrogen gas with a relative humidity (rH) of 50% could only be

measured with PTR-1. A comparison of the measurements under humid conditions was not possible, since the gas calibrator was only available at the lab container for the measurements with the PTR-1. The fraction of water clusters in the PTR-1 under dry conditions lied in the same range as in the other two PTR instruments, since a small amount of water vapour from the ion source can enter into the drift tube, and thus, some humidity is always present.

The relative abundances of the first water cluster $[H_2O]H_3O^+$ in PTR-2 and PTR-3 under dry conditions are around 1.5% and 0.9%, respectively. For the PTR-1, the relative abundance in the dry gas is only 0.13%. However, under humid conditions, an increase of the water cluster content to approximately 10% is observed, which is similar to the values reported by Pang.[24] It can also be observed that the second water cluster $[(H_2O)_2]H_3O^+$ (m/z 55.03897) has no significant contribution (0.017%) even under humid conditions.

3.1.2 | Nitrogen- and oxygen-derived ions

Back diffusion of nitrogen into the ion source can cause the formation of a series of different parasitic ions because of electron impact ionization, such as N_2^+ and N^{+}.[33] The N_3^+ and N_4^+ ions are subsequently
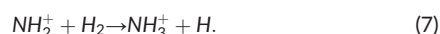
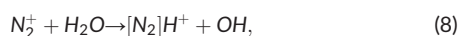formed and can be explained by the following intermolecular association reactions[34]:

$$N^+ + 2N_2 \rightarrow N_3^+ + N_2, \quad (2)$$

$$N_2^+ + 2N_2 \rightarrow N_4^+ + N_2. \quad (3)$$
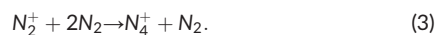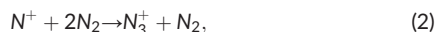
In the presence of hydrogen, the N_2^+ and N^+ ions can further react to[35]

$$N_2^+ + H_2 \rightarrow [N_2]H^+ + H, \quad (4)$$

$$N^+ + H_2 \rightarrow NH^+ + H. \quad (5)$$
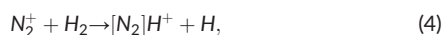
Subsequent reactions with hydrogen may lead to the products described in (6) and (7):

$$NH^+ + H_2 \rightarrow NH_2^+ + H, \quad (6)$$

$$NH_2^+ + H_2 \rightarrow NH_3^+ + H. \quad (7)$$
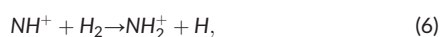
The reaction of these ions with water has been extensively discussed elsewhere.[34] In the presence of water, N_2^+ and N^+ ions can be transformed to[36]

$$N_2^+ + H_2O \rightarrow [N_2]H^+ + OH, \quad (8)$$

$$N_2^+ + H_2O \rightarrow H_2O^+ + N_2, \quad (9)$$

$$N^+ + H_2O \rightarrow H_2O^+ + N. \quad (10)$$
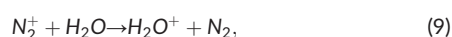
It has been shown that the ion $[N_2]H^+$ is produced according to Equation (8) with an ion distribution of about 18%.[33] The reaction of N^+ with NH_3 would produce the same ion with a yield of 9%.[34]

Besides Equations (4) and (8), the ion $[N_2]H^+$ can also be formed by the following reactions[34]:

$$NH^+ + N_2 \rightarrow [N_2]H^+ + N, \quad (11)$$

$$H_3^+ + N_2 \rightarrow [N_2]H^+ + H_2. \quad (12)$$
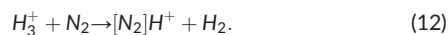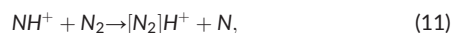
Reaction (11) is fast.[35] As pointed out by Milligan et al,[37] the $[N_2]H^+$ ion can influence the signal of alkanes, since the reaction rates of this ion with alkanes are faster than those with H_3O^+. Figure 2 shows the relative abundances of some parasitic ions found in the three PTR-TOF-MS instruments. Regarding the NO^+ and O_2^+ ions, which are the usual parasitic ions reported in literature,[3,4] their relative abundances in this study for all instruments were tuned to be below 0.2%.

Figure 2 indicates that the contribution of the parasitic ion $[N_2]H^+$ in relation to the H_3O^+ ion under dry conditions appears as the dominant ion species in PTR-1 followed by the $[NH_3]H^+$ ion. These ions occur with abundancies of around 14% and 4%, respectively. For the PTR-2 and PTR-3 instruments, the $[NH_3]H^+$ ion and the first water cluster, $[H_2O]H_3O^+$ (m/z 37.0284), exhibit the highest signals with contributions of around 1%. This suggests that the $[N_2]H^+$ ion is

mainly produced via protonation in the quadrupole interface of the PTR-1, although the proton affinity of nitrogen is quite low (494.88 kJ mol^{-1}). Thus, no significant competing reactions with VOCs are expected after its formation. In a similar manner, the formation of the $[CO_2]H^+$ ion has been ascribed to occur in the lower pressure, intermediate chamber between the drift tube and the mass spectrometer,[38] and the $[O_2]H^+$ ions have been ascribed to be formed from endothermic proton transfer reactions during ion extraction into the high-vacuum region.[39] The presence of the parasitic ion $[N_2]H^+$ was not reported in the article, in which the PTR-1 was introduced.[32] Moreover, in the presence of humidity, this ion can react with water according to (13) to produce H_3O^+ with a k rate of 2.6 × 10^{-9} cm^{-3} s^{-1}[37] (2.77 × 10^{-9} cm^{-3} s^{-1} and 5.5 × 10^{-9} cm^{-3} s^{-1})[34,36] and with an enthalpy of around −52 kcal mol^{-1} (−218 kJ mol^{-1}).

$$[N_2]H^+ + H_2O \rightarrow H_3O^+ + N_2. \quad (13)$$
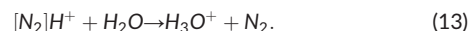
Nevertheless, the $[N_2]H^+$ ion is still produced in the ion source with relative ion abundancies of 0.3% and 0.17% for PTR-2 and PTR-3, respectively. In addition, humidity affects the $[N_2]H^+$ distribution in the PTR-1. The $[N_2]H^+$ species was reduced by approximately 80% at 50% rH at 20°C for N_2 5.0 and 6.0. For the $[NH_3]H^+$ ion, no clear humidity dependency was observed (Figure 3). The production of this parasitic ion in the ion source of PTR-MS instruments has been previously reported,[40] and it was found to be a very persistent ion. The presence of NH_3 in the pure nitrogen gases can be ruled out, since no decrease was observed after filtering nitrogen 6.0, showing a constant value of about 3.8%. The presence of the parasitic ion $[NH_3]H^+$ (NH_4^+) implies that ammonia is produced after successive hydrogenation reactions, and it is subsequently protonated inside the ion source before it is transferred into the drift tube. However, for a typical real gas analysis, background subtraction would eliminate the contribution of this ion. On the other hand, if ammonia is one of the target compounds, as it is known to be present in a variety of gases, such as coke oven gas[41,42] or biogases,[43] its presence in the background would worsen the detection limit.

Figure 3 shows the profile mass spectra of different nitrogen-containing parasitic ions in the different PTR devices. These ions are independent of the gas quality and, therefore, can be assigned to instrument artefacts. The corresponding ion intensities between PTR-2 and PTR-3 are similar except for N_2^+, indicating that comparable chemical processes regarding the formation of NH_2^+, NH_3^+, and $[NH_3]H^+$ (NH_4^+) ions occur in their ion sources. According to Adams et al,[44] the formation of the NH_4^+ ion in the presence of water from NH_3^+ is energetically unfavourable and proceeds with an efficiency of around 1%. This would support the hypothesis of ammonia formation prior to protonation. However, Adams et al[44] also show that the NH_4^+ ion can be formed by the following reaction:

$$NH_3^+ + NH_3 \rightarrow NH_4^+ + NH_2, \quad (14)$$
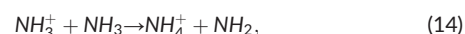
where the reaction can occur as either proton transfer from the NH_3^+ ion to the neutral NH_3 or through H-atom abstraction from the NH_3 by the NH_3^+. The findings shown in Figure 3B are somehow in contradiction because the humidity dependency observed for the NH_3^+ ion
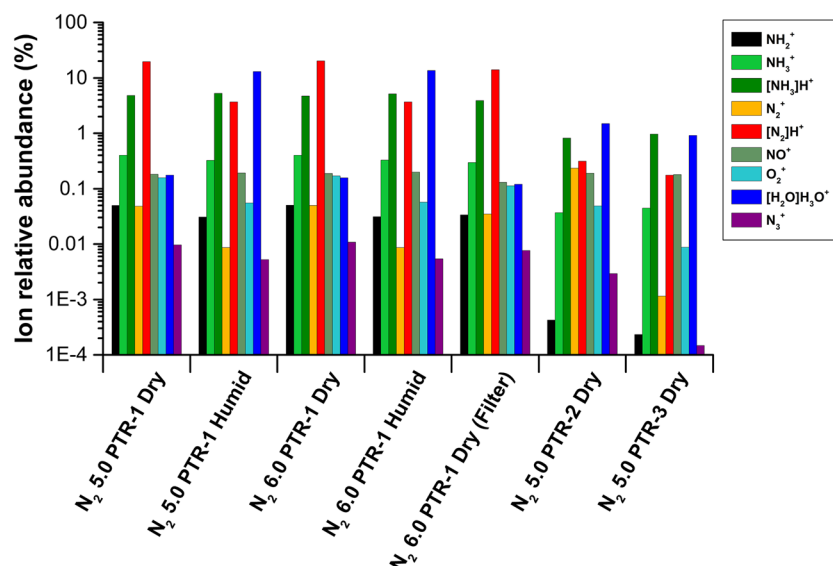
FIGURE 2 Measured ion distribution for typical parasitic ions observed under dry and humid conditions in three different PTR-TOF-MS instruments at E/N 131 using N_2 5.0 and 6.0 as carrier gas. PTR-TOF-MS, proton transfer reaction time-of-flight mass spectrometry
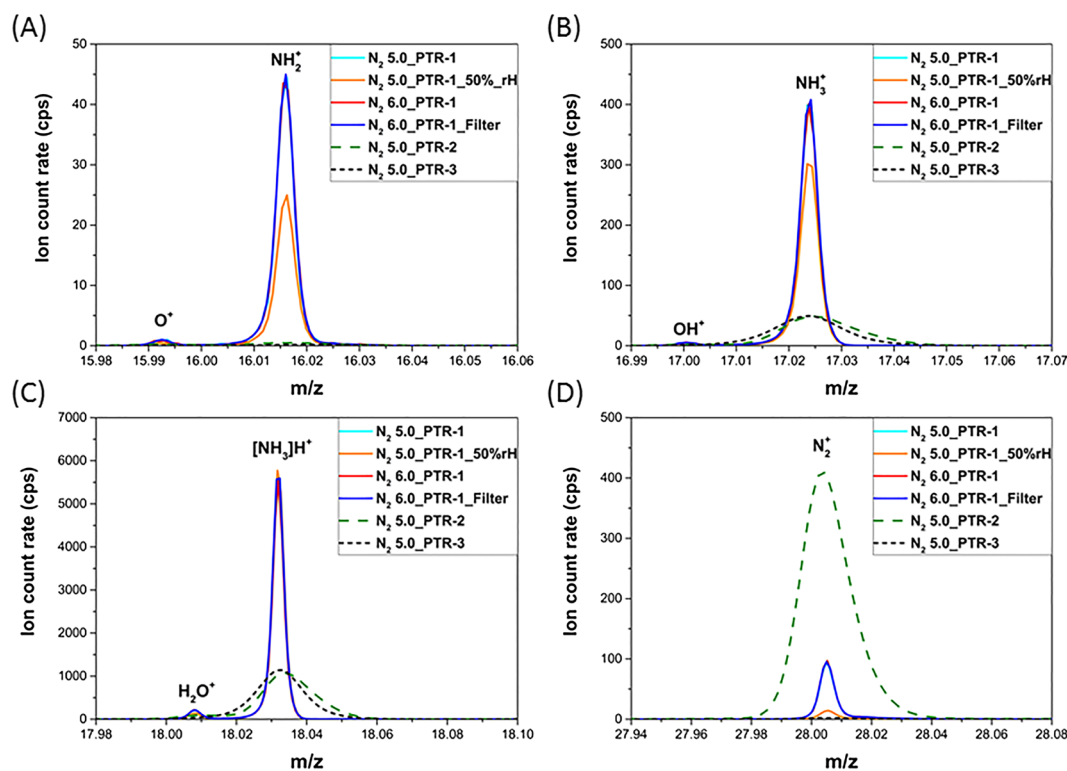

FIGURE 3 Comparison of the profile mass spectra of nitrogen-based parasitic ions (A) NH_2^+, (B) NH_3^+, (C) $[NH_3]H^+$, and (D) N_2^+) measured in the three PTR instruments. PTR, proton transfer reaction

is not reflected in the formation of the NH_4^+ ion. Assuming a solely protonation of NH_3 from H_3O^+, a concentration of 2.3 ppm and 816 and 857 ppb can be derived for the PTR-1, PTR-2, and PTR-3, respectively. These values are in contrast to the values reported by Norman et al,[40] who found NH_3 concentrations of about 100 ppb. The proton affinity of NH_3 (854.53 kJ mol^{-1}) is higher than that of most of the common VOCs, and therefore, only in a few cases it may compete with the H_3O^+ ion.

In contrast, PTR-2 exhibits a signal for N_2^+, which is 178 times higher than the signal found in PTR-3 and 6.5 times higher than in PTR-1. This indicates that the decay of this ion is more efficient in PTR-3 before leaving the ion source. For PTR-1, the signal intensities of the ions NH_2^+, NH_3^+, and N_2^+ depends on a certain extent on humidity. The content of these ions decreased with increasing rH content (50% rH at 20°C) by 38%, 18%, and 83%, respectively. With increasing rH of the inlet gas, back diffusion would promote reactions

(8) and (9), and thus, the H_2O^+ (Figure 3C) and $[N_2]H^+$ (Figure 4A) signals should increase. However, in the presence of humidity, a slight decrease is observed for the H_2O^+ ion, which can be explained by its consumption in the reaction with water molecules to form hydronium ions.

For $[N_2]H^+$ ions, reaction (13) can explain the significant reduction of this ion in the presence of water. For the determination of the $[N_2]H^+$ content in PTR-1, the mass of the second isotope at m/z 30.0105 ($[N_2]H^+(2)$) was used as the signal of the primary isotope at m/z 29.0134 ($[N_2]H^+(1)$) saturates. For PTR-2 and PTR-3, the first $[N_2]H^+$ isotope was used due to the overlapping of the second isotope with NO^+. Nevertheless, in the presence of humidity, this ion is expected to readily produce H_3O^+, which is based on Equation (13). Since this reaction is exothermic and this ion does not collide with VOC molecules in the quadrupole interface, no interference is expected.

In Figure 4A, it can be seen that PTR-2 and PTR-3 cannot resolve the peaks for NO^+ (m/z 29.9974) and $[N_2]H^+(2)$ (m/z 30.0105). As pointed out by Graus et al,[22] a resolution $m/\Delta m$ of at least 4000 to 5000 is needed in order to identify unknown substances by sum-formula assignments. Regarding the gas quality variation and the humidity change in PTR-1, the parasitic ion NO^+ did not show any variation. The formation of this ion has been described before.[33,34,45,46] From all possible reaction channels, NO^+ is probably produced to a major extend by the following reactions:

$$N^+ + O_2 \rightarrow NO^+ + O, \tag{15}$$

$$N_3^+ + O_2 \rightarrow NO^+ + N_2 + O, \tag{16}$$

$$O^+ + N_2 \rightarrow NO^+ + N. \tag{17}$$
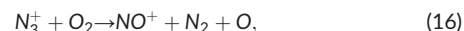
The formation of the NO^+ ion takes place exclusively in the ion source. Assuming that the nitrogen is only obtained by back diffusion from the inlet into the ion source, the required oxygen for the formation of NO^+ comes exclusively from the decomposition of water molecules. Thus, reaction (17) becomes the most significant source for NO^+. In the presence of humidity, the intensity of the O^+ ion drops by 60% as it is consumed by the reaction with water molecules. Consequently, a constant source of oxygen must be available in the ion source. Comparative measurements using air (Figure 4B) showed an increase of the signal of NO^+ by a factor of two. Thus, the increase of the NO^+ signal can only be assigned to reactions (15) and (16) as a result of the higher oxygen concentration and the presence of back diffusion. This is confirmed in Figure 4D, since O_2^+ can only be generated in the ion source but not in the drift tube.

For the parasitic ion O_2^+ (Figure 4C), its content clearly depends on humidity, which leads to a decrease of the signal of 65% in the presence of wet nitrogen gas. However, this ion is not consumed by the reaction with water molecules.[33] As N_2^+ and O^+ ions can react with oxygen to form O_2^+, competing reactions with water appear dominant in the system. Table 2 shows transmission corrected and normalized ion counts for the nitrogen-containing parasitic ions found in the
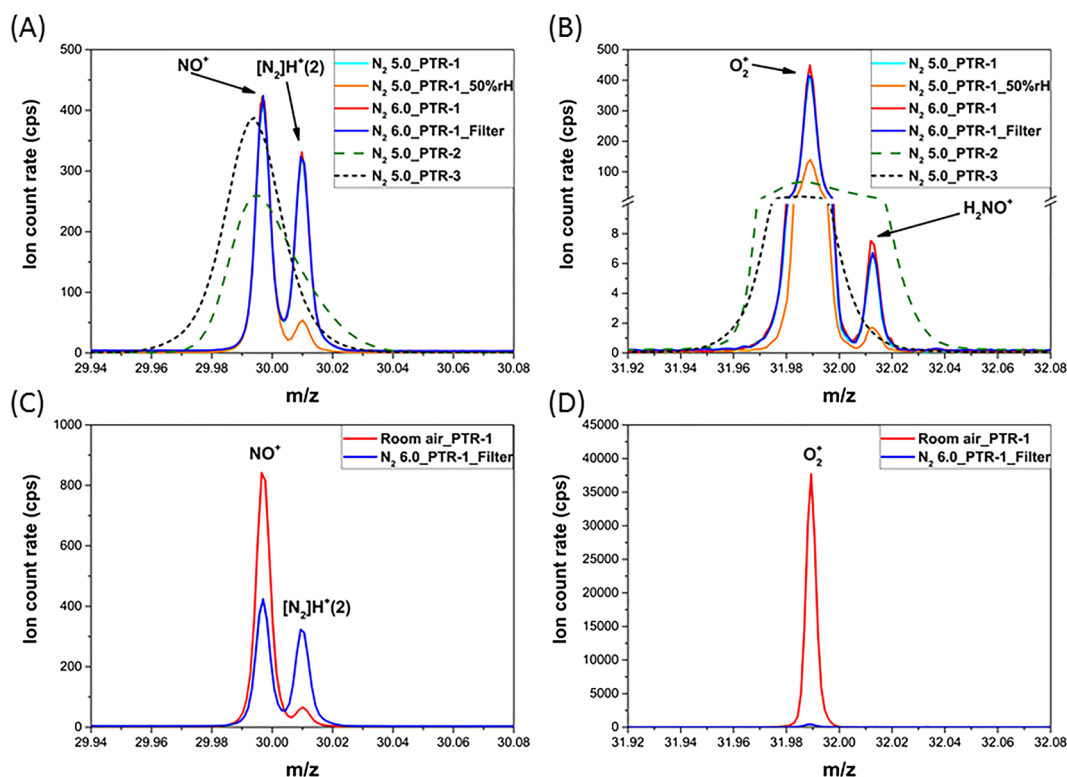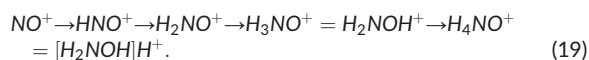

FIGURE 4 Measured ion distribution for the typical parasitic ions NO^+ and O_2^+ observed under dry and humid conditions in three different PTR instruments (A) and (C). Comparative measurement with room air (B) and (D) using PTR-1. PTR, proton transfer reaction

measurements with N_2 5.0 and 6.0 under dry and humid conditions. Apart from the trend observed for hydrogenated N^+ species:

$$N^+ \rightarrow NH^+ \rightarrow NH_2^+ \rightarrow NH_3^+ \rightarrow NH_4^+, \tag{18}$$
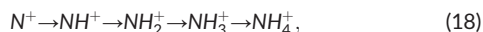
a similar trend was observed for NO^+:

$$NO^+ \rightarrow HNO^+ \rightarrow H_2NO^+ \rightarrow H_3NO^+ = H_2NOH^+ \rightarrow H_4NO^+$$
$$= [H_2NOH]H^+. \tag{19}$$

Although in both cases, the last step corresponds rather to a protonation. The presence of the HNO^+ (or NOH^+) ion is rather surprising, since the reaction of NO^+ with hydrogen was shown to be ineffective.[35] Ions such as H_2NO^+ have been reported before in a selected ion flow tube (SIFT)[33] with a 100% selectivity in the reaction with water molecules:

$$N_3^+ + H_2O \rightarrow H_2NO^+ + N_2. \tag{20}$$
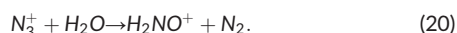
In addition, the reaction rate constant for the formation of the H_2NO^+ ion has been shown to be rather small (2.57×10^{-10} cm^{-3} s^{-1}).[34] To our knowledge, the H_2NOH^+ ion or the subsequent protonated form $[H_2NOH]H^+$ have not been observed before in PTR measurements. Müller et al.[47] reported a peak at m/z 33.0204 as $DNOH^+$, and it was assigned as instrumental background. That also applies for $[H_2N_2]H^+$ (m/z 31.0291), N_3^+ (m/z 42.0087), HN_3^+ (m/z 43.0165), and $[HN_3]H^+$ (m/z 44.0243). These ions could be identified thanks to the higher resolution of PTR-1 in comparison with the instruments used in the literature. Moreover, because of the lower resolution of those instruments, the overlapping of peaks could not be resolved, so that in the interpretation of the mass spectra, the ions identified in this study were overseen.

Other ions shown in Table 2 such as, the N_2OH^+ ion, have a low reaction rate constant of formation with H_2 as reported using a flowing-afterglow reaction tube.[35] The formation of this ion in the PTR-1 instrument is more likely attributable to the proton transfer reaction from the $[N_2]H^+$ ion. A similar kind of protonation for endothermic reactions has been observed for CO_2.[38] In general, most of the ions reported here have been shown to be present in astrophysical environments.[48,49]

In contrast to PTR-2 and PTR-3, PTR-1 is able to resolve four peaks around m/z 31 (Figure 5A). The PTR-3 exhibits a contribution of mainly $NO^+(2)$, whereas PTR-2 exhibits an additional signal that corresponds to formaldehyde. The presence of the ion $[H_2N_2]H^+$ has not been reported before in the PTR literature. This ion exhibits a very small positive humidity dependency. In contrast, the HNO^+ ion shows a signal decrease of about 66% in the presence of humidity. This can be attributed to its consumption in the formation of the H_2NO^+ and H_2NOH^+ ions. Since the nitrogen gas used for the measurements in both, PTR-2 and PTR-3, was the same (N_2 5.0 from supplier B), the presence of formaldehyde in PTR-2 can be attributed to memory effects. Thus, formaldehyde is not present in this nitrogen gas or at least at a level that is not detectable by PTR-3. For PTR-3 as a new instrument, wall adsorption effects could play a role, since potential
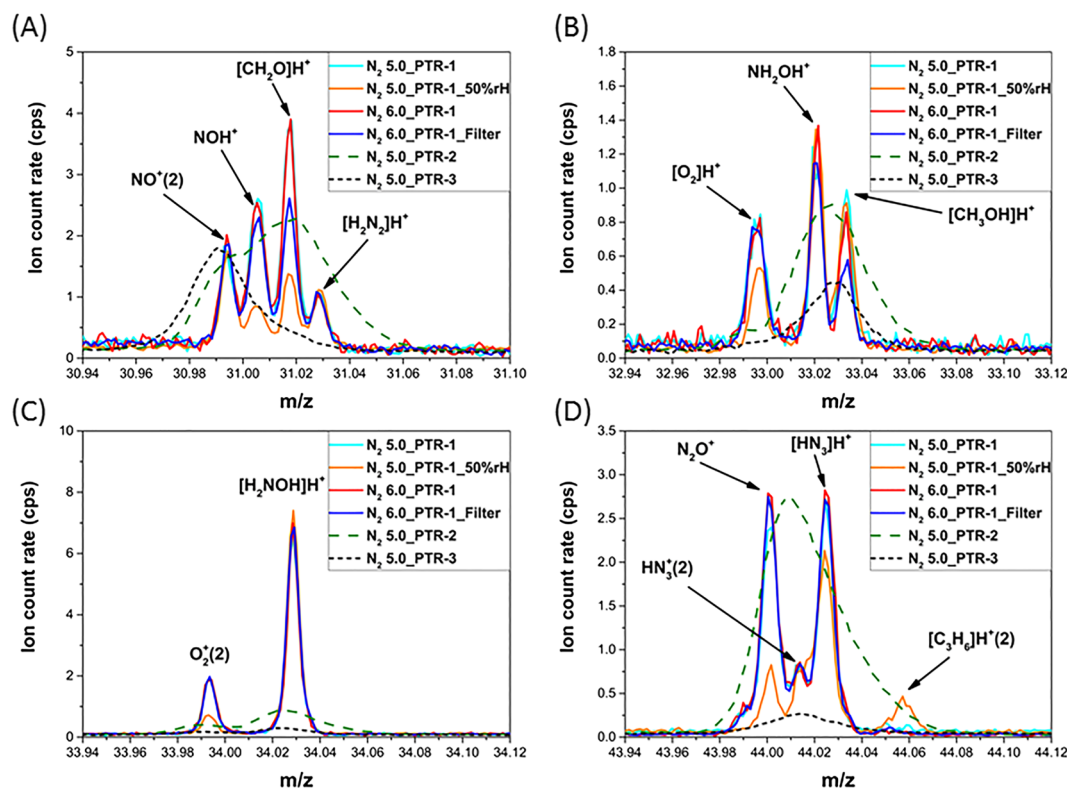

FIGURE 5 Measured ion count rates of minor parasitic ions and relevant VOCs observed under dry and humid conditions in three different PTR instruments. (A) Formaldehyde, (B) methanol, (C) $[H_2NOH]H^+$, and (D) N_2O^+ and $[HN_3]H^+$. PTR, proton transfer reaction; VOC, volatile organic compound

adsorbing surfaces are still clean. Hence, formaldehyde could be removed from the N_2, by adsorption on specific surfaces to a certain extend until saturation takes place. Furthermore, the measurements conducted with the PTR-1 reveal no significant difference between nitrogen samples with different gas qualities (N_2 5.0 and 6.0, from supplier A). After filtering N_2 6.0, a decrease of the formaldehyde content of about 20% is observed. This indicates the presence of formaldehyde in these gases (supplier A). Previous reports have shown that if the occurrence of formaldehyde would be due to a memory effect, the signal in the dry and filtered gas should be higher, since a dry gas improves the sensitivity towards formaldehyde.[50] With increasing humidity, the back reaction becomes more significant, as a result of the rather low exothermicity (about 5 kcal mol^{-1}) of the protonation reaction.[50,51] A humidity dependence on sensitivity has also been shown by Inomata et al.[52] and Vlasenko et al.[53] In their reports, a reduction of almost 72% in the formaldehyde signal is observed in the gas measured at a rH of 50% at 20°C. In this study, the reduction of formaldehyde under humid conditions accounted for about 68% and 64% for N_2 5.0 and 6.0 (from supplier A), respectively.

The methanol signal in the PTR-1 is shown in Figure 5B. No clear dependency on the humidity can be observed. This is in agreement with previous results.[50] In the filtered gas sample, the methanol signal decreases by 34%. This indicates methanol is a VOC impurity but can be present as memory effect. In Figure 5B, it can be seen that the PTR-2 and PTR-3 do not resolve the peak at m/z 33. Only PTR-1 reveals an interference with the NH_2OH^+ ion, which to our knowledge, until now has not been reported. In general, all instruments exhibit a signal for methanol, which interferes with the isobaric NH_2OH^+ ion. For methanol analysis, this kind of interference has not been reported before in the literature.[9,20] However, the interference of the protonated molecular oxygen ion, $[O_2]H^+$, has been shown for the m/z 33.[39]

Figure 5 shows that instrumental parasitic ions can be identified, since they are independent of the gas quality. However, some of them exhibit a negative humidity dependency like NOH^+ (Figure 5 A), $[O_2]H^+$ (Figure 5B), N_2O^+, and $[HN_3]H^+$ (Figure 5D). The protonated hydroxylamine ion $[NH_2OH]H^+$ shows no humidity dependency, and as expected for a parasitic ion, the filtering has no effect on it (Figure 5C). Its formation remains unclear and is not the scope of this study. Figure 5D shows the presence of three isobaric ions at m/z 44. Both PTR-2 and PTR-3 instruments exhibit a signal around this mass but are not able to resolve it. Some of the parasitic ions observed in PTR-1 are possibly not present in the PTR-2 and PTR-3 instruments. The N_2O^+ ion can be assigned as artefact because of its nearly constant signal in N_2 5.0, 6.0, and after filtering. However, it shows a clear negative humidity dependency, which accounts for a signal drop of about 71% and 78% in N_2 5.0 and 6.0, respectively. The $[HN_3]H^+$ ion in Figure 5D is isobaric with ionized acetaldehyde ($C_2H_4O^+$). However, the $C_2H_4O^+$ ion can be ruled out, since the protonated acetaldehyde at m/z 45 (not shown here) decreases after filtering N_2 6.0. This indicates the presence of acetaldehyde in the gas as a trace contaminant rather than the occurrence of memory effects or instrument artefacts. The $[HN_3]H^+$ ion shows a

slight decrease of the signal with increasing humidity, accounting for a reduction of about 0.6 and 2.5% for N_2 5.0 and 6.0, respectively. The usually reported[54] ion of the isocyanic acid, $[HNCO]H^+$, at m/z 44.0131 can be ruled out, since it easily undergoes hydrolysis, and therefore, it would be strongly humidity dependent, which was not observed. This peak has been assigned to the second most abundant isotope of the HN_3^+ ion (m/z 44.0135), which to our knowledge has not been reported in PTR measurements. Based on these findings, another sequence can be assigned for the N_3^+ ion:

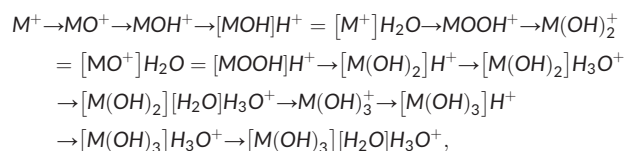$$N_3^+ \rightarrow HN_3^+ \rightarrow H_2N_3^+ = [HN_3]H^+. \tag{21}$$
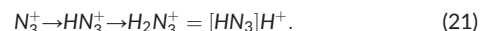
According to de Gouw and Warneke,[12] ligand switching reactions are probably a more general mechanism for causing a humidity dependent sensitivity. This is very important, since in the measurement of catalytic processes, the background is usually measured with the purging dry gas (eg, Ar or N_2) at the beginning of the reaction. Under reaction conditions, the water content may change, and consequently, an artefact can exhibit an increase or decrease of the signal by an order of magnitude. This would complicate the background subtraction during the data processing.

3.2 | Minor parasitic ions

3.2.1 | Metal-containing ions

In the analysis of industrial process gases or products of heterogeneous catalytic reactions, metal-containing compounds can be found.[55] Iron- or nickel-based materials are commonly used as catalysts or in purification processes. Thus, special attention was set to the presence of possible metal-containing ions in background measurements, which could interfere with metal-containing compounds in the real industrial process gases. Figures 6–8 show some metal species from Cr^+, Fe^+, and Ni^+, respectively, and a few of their reaction products. These ions are assigned to originate from the ion source as a consequence of the electron bombardment on metal surfaces. Because these metal ions are independent of the buffer gas used, they can be easily assigned as instrument artefacts. All species found are given in Table 3. The following reaction sequence was observed for these metal ions:

$$\begin{aligned} M^+ \rightarrow MO^+ &\rightarrow MOH^+ \rightarrow [MOH]H^+ = [M^+]H_2O \rightarrow MOOH^+ \rightarrow M(OH)_2^+ \\ &= [MO^+]H_2O = [MOOH]H^+ \rightarrow [M(OH)_2]H^+ \rightarrow [M(OH)_2]H_3O^+ \\ &\rightarrow [M(OH)_2][H_2O]H_3O^+ \rightarrow M(OH)_3^+ \rightarrow [M(OH)_3]H^+ \\ &\rightarrow [M(OH)_3]H_3O^+ \rightarrow [M(OH)_3][H_2O]H_3O^+, \end{aligned}$$

where M is any transition metal (Cr, Fe, Ni, etc). For PTR-1, humidity positively influences the last two reaction steps, while for all other steps, humidity causes a decrease of the corresponding signal. Ions showing a decreasing signal with humidity are thought to act as intermediates, whereas those ions exhibiting positive dependency act as final products. To our knowledge, this kind of trend has not been reported before in PTR-instruments.

FIGURE 6 Measured ion count rates of chromium ion and some of its oxidation and hydration species observed under dry and humid conditions in three different PTR-TOF-MS instruments. (A) Cr^+, (B) $[CrOH]H^+$, (C) $[CrOOH]H^+$, and (D) $[Cr(OH)_3]H_3O^+$. PTR-TOF-MS, proton transfer reaction time-of-flight mass spectrometry

FIGURE 7 Measured ion count rates of iron ion and some of its oxidation and hydration species observed under dry and humid conditions in three different PTR-TOF-MS instruments. (A) Fe^+, (B) FeO^+/$[FeOH]H^+(2)$, (C) $[FeOOH]H^+$, and (D) $[Fe(OH)_3]H_3O^+$. PTR-TOF-MS, proton transfer reaction time-of-flight mass spectrometry
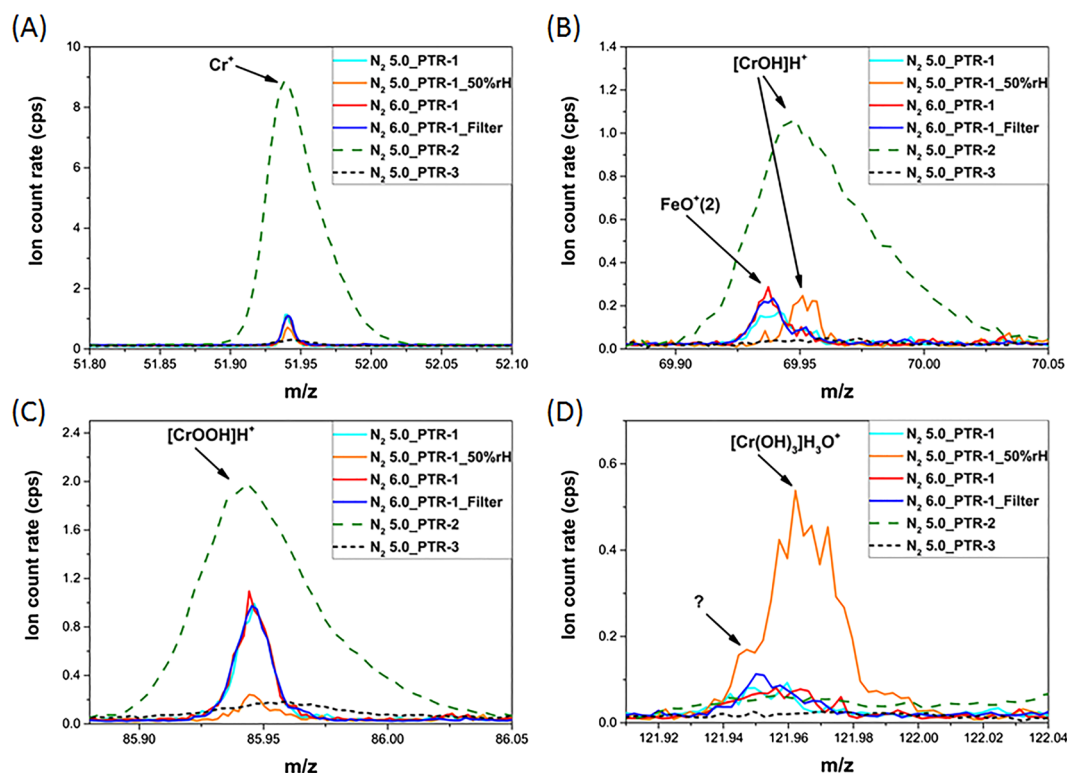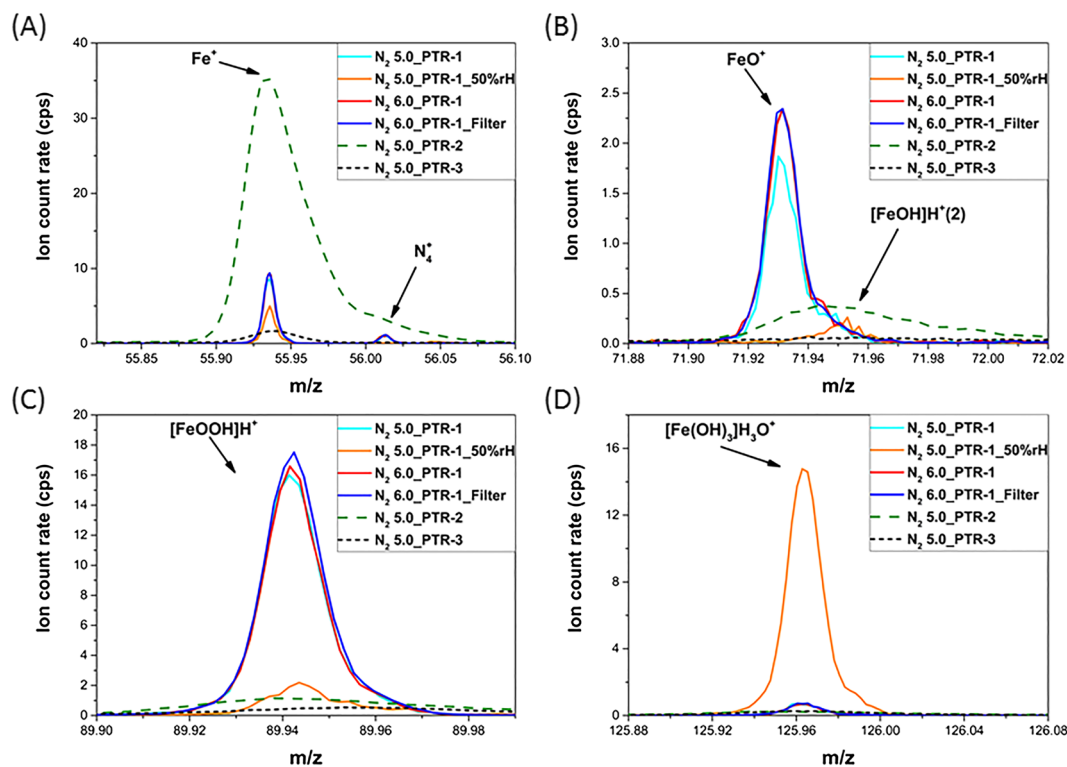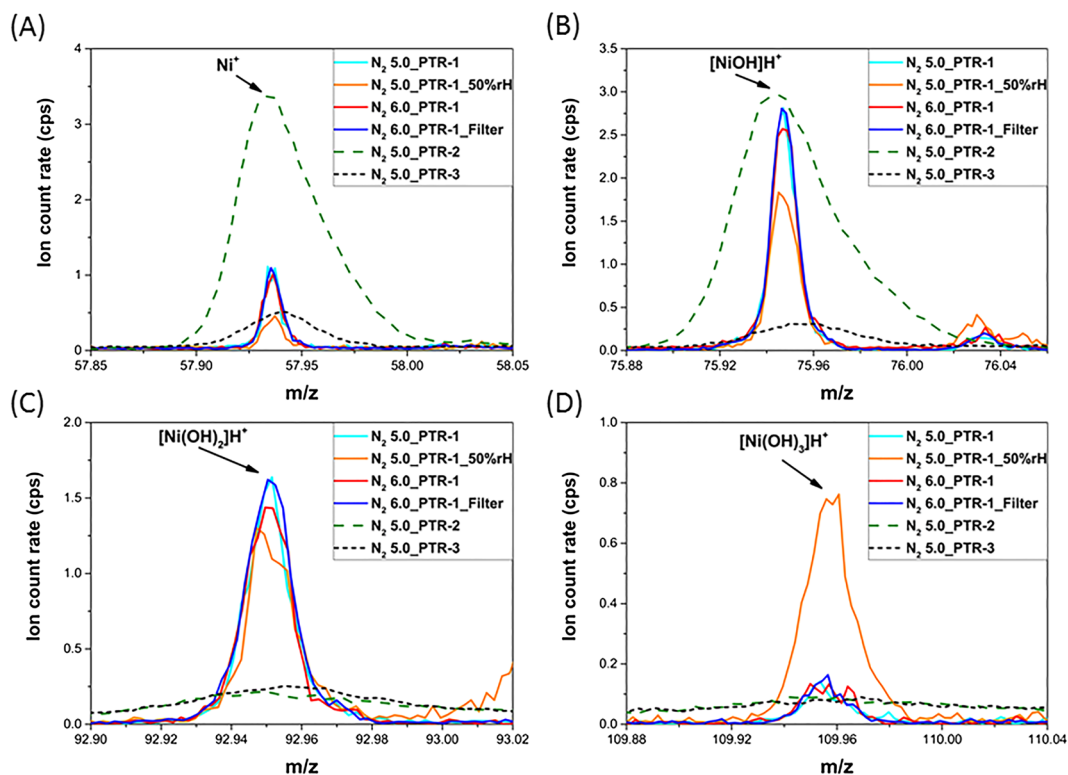
FIGURE 8 Measured ion count rates of nickel ion and some of its oxidation and hydration species observed under dry and humid conditions in three different PTR-TOF-MS instruments. (A) Ni^+, (B) $[NiOH]H^+$, (C) $[Ni(OH)_2]H^+$, and (D) $[Ni(OH)_3]H^+$. PTR-TOF-MS, proton transfer reaction time-of-flight mass spectrometry

TABLE 3 Transmission corrected and normalized ion count rates of minor metal-containing ions observed under dry and humid conditions in three different PTR instruments using N_2 5.0 and 6.0

Measured mass at PTR-1 (m/z)	Theoretical mass (m/z)	Chemical formula (tentative assignment)	N_2 5.0 PTR-1 Dry (ncps)	Humid (ncps)	N_2 6.0 PTR-1 Dry (ncps)	Humid (ncps)	N_2 6.0 PTR-1 Filter Dry (ncps)	N_2 5.0 PTR-2 Dry (ncps)	N_2 5.0 PTR-3 Dry (ncps)
51.9411	51.9400	Cr^+	1.604	1.141	1.874	1.254	1.720	63.745	1.864
54.9384	54.9375	Mn^+	0.278	0.390	0.281	0.409	0.298	4.026	0.794
55.9355	55.9344	Fe^+	13.281	7.261	14.061	7.673	14.231	227.589	6.414
57.9361	57.9348	Ni^+	2.161	0.952	2.212	1.051	2.054	29.069	3.166
58.9312	58.9306	Co^+	0.038	0.026	0.049	0.062	0.036	1.965	0.605
62.9308	62.9291	Cu^+	0.099	0.129	0.112	0.115	0.130	1.787	0.700
63.9284	63.9286	Zn^+	0.077	0.050	0.081	0.159	0.053	0.000	0.000
66.9392	66.9383	VO^+	0.018	0.016	0.018	0.024	0.017	0.905	0.592
67.9365	67.9349	CrO^+	0.152	0.031	0.168	0.046	0.142	0.766	0.388
68.9440	68.9427	$CrOH^+$	0.084	0.049	0.110	0.045	0.134	0.763	0.434
69.9516	69.9505	$[CrOH]H^+$	0.082	0.366	0.081	0.376	0.077	7.029	0.335
71.9314	71.9293	FeO^+	2.269	0.045	2.869	0.065	2.838	0.801	0.228
72.9391	72.9371	$FeOH^+$	8.110	3.283	8.900	3.329	8.813	13.669	2.787
73.9288	73.9297	NiO^+	0.251	0.256	0.307	0.273	0.358	0.000	0.000
73.9462	73.9450	$[FeOH]H^+$	1.793	4.303	1.913	4.327	1.842	26.336	1.338
74.9398	74.9375	$NiOH^+$	0.335	0.202	0.376	0.202	0.415	0.000	0.000

(Continues)

TABLE 3 (Continued)

Measured mass at PTR-1 (m/z)	Theoretical mass (m/z)	Chemical formula (tentative assignment)	N₂ 5.0 PTR-1		N₂ 6.0 PTR-1		N₂ 6.0 PTR-1 Filter	N₂ 5.0 PTR-2	N₂ 5.0 PTR-3
			Dry (ncps)	Humid (ncps)	Dry (ncps)	Humid (ncps)	Dry (ncps)	Dry (ncps)	Dry (ncps)
75.9473	75.9454	$[NiOH]H^+$	4.418	3.580	4.455	3.513	4.538	19.557	2.065
80.9418	80.9396	$[CuOH]H^+$	0.164	0.141	0.133	0.136	0.133	0.273	0.164
81.9395	81.9392	$[ZnOH]H+$	0.115	0.101	0.160	0.134	0.146	0.399	0.000
84.9399	84.9376	$[CrOO]H^+$	0.859	0.393	0.971	0.287	1.113	0.789	0.000
85.9458	85.9454	$[CrOOH]H^+$	1.116	0.218	1.075	0.236	1.261	9.562	1.027
88.9356	88.9320	$[FeOO]H^+$	0.670	0.155	0.738	0.185	0.746	1.048	0.270
89.9423	89.9399	$[FeOOH]H^+$	17.831	1.782	18.139	1.688	18.811	5.437	2.048
89.9543	89.9508	$[Mn(OH)_2]H^+$	4.662	1.116	7.066	1.343	5.956	0.000	0.000
90.9499	90.9477	$[Fe(OH)_2]H^+$	25.593	20.089	25.860	20.043	26.396	55.584	17.397
91.9415	91.9403	$Ni(OH)_2^+$	0.790	0.304	0.829	0.475	0.864	7.062	0.838
92.9508	92.9481	$[Ni(OH)_2]H^+$	2.127	1.368	2.244	2.006	2.332	1.537	1.243
93.9571	93.9559	$[NiOH]H_3O^+$	2.280	5.093	2.318	5.257	2.288	4.496	0.746
94.9527	94.9538	$[CoOH]H_3O^+$	0.187	0.200	0.168	0.240	0.296	0.134	0.096
98.9493	98.9502	$[CuOH]H_3O^+$	0.113	0.158	0.118	0.141	0.115	0.170	0.138
99.9370	99.9360	$[VO_3]H^+$	0.132	0.015	0.172	0.026	0.189	0.000	0.000
99.9484	99.9497	$[ZnOH]H_3O^+$	0.162	0.131	0.159	0.128	0.208	0.000	0.000
101.9409	101.9404	$CrO(OH)_2^+$	1.504	0.599	1.483	0.536	1.506	0.281	0.077
102.9501	102.9482	$Cr(OH)_3^+$	1.949	1.758	1.928	1.721	2.297	1.968	0.832
103.9551	103.9560	$[Cr(OH)_3]H^+$	0.430	0.439	0.476	0.489	0.484	6.947	0.745
103.9670	103.9673	$[V(OH)_2]H_3O^+$	1.006	1.557	1.046	1.596	0.891	0.000	0.000
104.9632	104.9638	$[Cr(OH)_2]H_3O^+$	0.039	0.126	0.046	0.097	0.043	0.232	0.057
105.9338	105.9348	$FeO(OH)_2^+$	0.608	0.337	0.638	0.385	0.563	0.215	0.052
105.9455	105.9457	$Mn(OH)_3^+$	0.266	0.175	0.269	0.175	0.271	0.147	0.044
106.9454	106.9426	$Fe(OH)_3^+$	1.139	0.933	1.178	0.825	1.146	0.000	0.000
107.9530	107.9504	$[Fe(OH)_3]H^+$	5.842	10.147	5.296	9.819	5.643	1.988	1.495
108.9599	108.9583	$[Fe(OH)_2]H_3O^+$	1.342	12.618	1.202	13.277	1.188	2.822	1.223
109.9550	109.9508	$[Ni(OH)_3]H+$	0.190	1.307	0.207	1.280	0.188	0.339	0.246
110.9605	110.9587	$[Ni(OH)_2]H_3O^+$	0.098	1.055	0.115	1.089	0.099	0.000	0.000
111.9569	111.9565	$[Co(OH)_2]H_3O^+$	0.027	0.096	0.029	0.116	0.050	0.000	0.000
115.9495	115.9446	$[Zn(OH)_3]H+$	0.234	0.023	0.249	0.068	0.259	0.000	0.000
116.9525	116.9525	$[Zn(OH)_2]H_3O^+$	0.070	0.091	0.063	0.044	0.099	0.192	0.132
119.9526	119.9509	$[CrO_2OH]H_3O^+$	2.155	4.131	2.171	4.450	2.362	0.301	0.225
120.9603	120.9587	$[CrO(OH)_2] H_3O^+$	0.162	1.338	0.160	1.223	0.147	0.000	0.000
121.9647	121.9666	$[Cr(OH)_3]H_3O^+$	0.022	0.681	0.037	0.445	0.029	0.000	0.000
124.9521	124.9532	$[FeO(OH)_2]H_3O^+$	0.107	0.650	0.099	0.891	0.104	0.000	0.000
124.9597	124.9641	$[Mn(OH)_3]H_3O^+$	0.029	0.824	0.054	0.438	0.054	0.000	0.000
125.9637	125.9610	$[Fe(OH)_3]H_3O^+$	0.672	14.392	0.630	14.627	0.652	0.438	0.351
126.9699	126.9688	$[Fe(OH)_2][H_2O]H_3O^+$	0.043	1.473	0.030	1.576	0.028	0.338	0.317
127.9605	127.9614	$[Ni(OH)_3]H_3O^+$	0.007	0.232	0.026	0.254	0.016	0.000	0.000
128.9678	128.9692	$[Ni(OH)_2][H_2O]H_3O^+$	0.067	0.107	0.026	0.131	0.013	0.136	0.124

(Continues)

TABLE 3 (Continued)

Measured mass at PTR-1 (m/z)	Theoretical mass (m/z)	Chemical formula (tentative assignment)	N₂ 5.0 PTR-1		N₂ 6.0 PTR-1		N₂ 6.0 PTR-1 Filter	N₂ 5.0 PTR-2	N₂ 5.0 PTR-3
			Dry (ncps)	Humid (ncps)	Dry (ncps)	Humid (ncps)	Dry (ncps)	Dry (ncps)	Dry (ncps)
139.9714	139.9771	$[Cr(OH)_3][H_2O]H_3O^+$	0.008	0.0057	0.003	0.075	0.004	0.076	0.068
142.9704	142.9746	$[Mn(OH)_3][H_2O]H_3O^+$	0.012	0.084	0.007	0.053	0.002	0.077	0.031
143.9292	143.9306	$[PrH_2]H^+$	0.264	0.299	0.353	0.496	0.275	0.135	0.063
143.9699	143.9716	$[Fe(OH)_3][H_2O]H_3O^+$	0.017	0.142	0.038	0.189	0.017	0.107	0.065

Abbreviations: n.d., not determined; PTR, proton transfer reaction.

3.2.2 | Chromium species

Figure 6A shows that in the case of chromium (Cr^+) for PTR-2, in comparison with the newer PTR-3, it exhibits an almost 30 times higher signal. This may suggest some kind of aging process occurring in the ion source. Although the composition of the stainless steel metal surfaces in the ion source are unknown, this metal surface appears as the only plausible source of chromium. PTR-1 showed in general low signals towards chromium species. Under dry conditions, PTR-3 and PTR-1 exhibit similar values. In the presence of humidity, the ion signal decreases about 23% in PTR-1, which can be assigned to subsequent reactions with oxygen or water molecules. All chromium intermediates (see Table 3) show a decrease with humidity except for the $[CrOH]H^+$ ion (m/z 69.9505), which exhibits a signal 3 times higher compared with dry conditions. However, at this stage, it remains unclear if the assigned ion really forms or instead the association ion $[Cr^+]H_2O$ is the species observed. In contrast to iron (Figure 7) and nickel (Figure 8), the protonated chromium (III) hydroxide ($[Cr(OH)_3]H^+$) did not show a clear humidity dependency. The presence of this ion confirms the occurrence of the proposed subsequent reactions. The association ions $[Cr(OH)_3]H_3O^+$ (Figure 6D) and $[Cr(OH)_3][H_2O]H_3O^+$ (Table 3) showed under humid conditions in PTR-1 a signal increase of almost 8 and 11 times, respectively. The $[CrOOH]H^+$ ion (m/z 85.9454) exhibited a negative humidity dependency with a signal drop of about 80% for N₂ 5.0 and 78% for N₂ 6.0. This signal decrease is assigned to its consumption in subsequent reactions with for instance water molecules. The exact nature of this ion remains unclear since the isomeric ion $[CrO^+]H_2O$ could also be possible. However, if the formation of the association ion was the reaction taking place in the system, it would be expected that the intensity increases with humidity, because of the higher number of water molecules available.

3.2.3 | Iron species

Similar to chromium, the iron ion (Fe^+) shown in Figure 7A exhibited a signal in PTR-2 30 times higher than in PTR-3, which is presumed to be due to aging of the ion source. This signal increase can be used as an indicator of aging. Until now, the usual procedure for checking the aging of the ion source is to follow the drop in sensitivity of the VOCs of interest, which has to be compensated by increasing the current in the ion source. Figure 7B shows a decrease of about 98% for the FeO^+ ion in the presence of humidity in the PTR-1. By comparing the N₂ 5.0 with 6.0, it can be seen that this ion exhibits a signal drop of about 20% in N₂ 5.0 compared with N₂ 6.0. This effect can be ascribed to the higher water content in N₂ 5.0. The $[Fe(OH)_3]H^+$ ion (Table 3) shows an increase of about 1.6 times under humid conditions, but the association ions $[Fe(OH)_2]H_3O^+$ and $[Fe(OH)_3]H_3O^+$ exhibited an increase of about 9 times and 22 times, respectively. This positive humidity dependency is expected since these ions are not expected to further react and therefore, act as final products in the sequence shown in Equation (22). The $[FeOOH]H^+$ ion (Figure 7C) showed, in agreement with the equivalent chromium species a signal drop under humid conditions of about 90%, which again is assigned to its consumption in subsequent reactions.

From all metal-containing ions, the highest contribution in the mass spectra was ascribed to the $[Fe(OH)_2]H^+$ ion in the PTR-3 and in the PTR-1 with relative ion abundances of 0.002% and 0.003%, respectively. Only in the PTR-2, the Fe^+ ion appeared as dominant metal species (0.023%) followed by the $[Fe(OH)_2]H^+$ ion (0.006%).

3.2.4 | Nickel species

In general, nickel species showed a similar trend like iron. Figure 8A shows that the Ni^+ ion (m/z 57.9348) exhibited in PTR-2 a 9 times higher signal than in PTR-3. In the presence of humidity, the Ni^+ ion showed an ion intensity decrease of 56% in PTR-1, as a consequence of its consumption in subsequent reactions. Figure 8B shows that signal intensity of the $[NiOH]H^+$ ion decreases by about 19% in the presence of humidity. In a similar fashion like chromium or iron ions, this ion reacts possibly with water molecules following the sequence in Equation (22). The $[Ni(OH)_2]H^+$ ion (Figure 8C) showed no clear trend and its lower signal under humid conditions may indicate its consumption in further reactions. In summary, the metal-containing ions exhibit relative ion abundances below 0.01% in all instruments. Because of the fact that the tentative assignment of chemical formulas could be associated to different isomeric species, deeper investigations are needed. Moreover, some theoretical calculations are planned in order
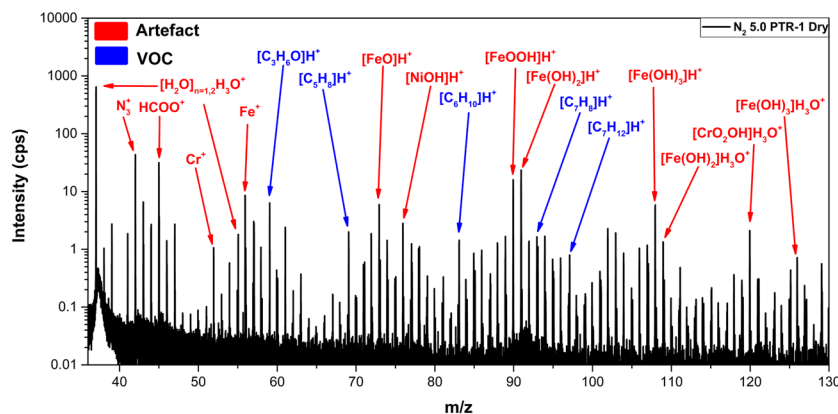
FIGURE 9 Average mass spectrum from a background measurement using nitrogen 5.0 under dry conditions for the m/z range 36 to 130 with the PTR-1. PTR, proton transfer reaction

to clarify the probability of formation of some ions or clusters (association ions).

Table 3 shows a complete list of the main isotopes of metal-containing ions, which could be identified as instruments artefacts. Tentative chemical formulas were assigned to the peaks found in the mass spectra of background measurements using N2 5.0 and 6.0 under dry and humid conditions. It became clear that most of these parasitic ions exhibited a humidity dependency. This could be quite helpful because ions that apparently cannot be sensed under dry conditions are measurable in the presence of humidity.

3.3 | Implications on full spectra

If PTR-TOF-MS is applied for the trace analysis of complex gas mixtures like metallurgical gases (coke oven gas, blast furnace gas, and basic oxygen furnace gas), the contribution of the instrument artefacts as well as the VOCs in the diluent have to be considered. This is required for a correct interpretation of the obtained spectra as these gases usually have to be strongly diluted before analysis. Figure 9 shows an average mas spectrum obtained from the measurement of nitrogen 5.0 under dry conditions in the PTR-1. At first glance, it becomes clear that the amount and intensities of artefacts at the trace level are quite significant and therefore, their differentiation from real VOCs has to be done in order to avoid possible misinterpretations or, in the case of humidity dependent artefacts, even misestimations. In Figure 9, ion masses at m/z 37 and 55 correspond to the first and second hydronium-water clusters, respectively. In the m/z range 36 to 130, the second and third most intense peaks were assigned to the N_3^+ ion at m/z 42, followed by the $HCOO^+$ ion at m/z 45. However, when CO_2 is present in the gas matrix, the formation of the protonated ion $[CO_2]H^+$ at m/z 45 is also possible.[38] Among the metal-containing species, the $[Fe(OH)_2]H^+$ ion at m/z 91 exhibited the highest intensity. Figure 9 shows that many metal-containing ions contribute to the background signals. Because most of them exhibit a humidity dependency, their complete elimination by background subtraction might be difficult, but for a meaningful analysis of complex gas mixtures, their contribution has to be incorporated in the interpretation of the obtained results.

4 | CONCLUSIONS

A straightforward methodology was introduced in order to identify instrumental artefacts in PTR-MS analysis. Parasitic ions, memory effects, and real trace impurities can be identified during background measurements when using conventional inert gases, such as nitrogen. It was found that instrumental parasitic ions are independent of the gas quality used, which enables their differentiation from real VOCs. Their intensities still may depend in some cases on the water content in the different gas qualities and in the system, and thus, their humidity dependency can further complicate the interpretation of the mass spectra. For the applied PTR instruments, the parasitic ions NO^+ and O_2^+ were not dominant, exhibiting ion signals below 0.2%. In contrast, the signal was dominated by $[N_2]H^+$ and $[NH_3]H^+$ ions, which were determined in the spectrum of the PTR-1 under dry conditions with ion abundances of about 14% and 4%, respectively. In the presence of humidity, the $[N_2]H^+$ ion decreases strongly to about 2.7%, whereas the $[NH_3]H^+$ ion shows no clear humidity dependency and stays almost constant around 4%. On the other hand, the first water cluster appears as the dominant parasitic ion with an increase from 0.2% up to 13%, when increasing the rH up to 50% at 20°C. Both PTR-2 and PTR-3 instruments showed no significant contribution of the $[N_2]H^+$ ion, which supports the idea of $[N_2]H^+$ formation in the quadrupole interface of PTR-1. The methodology presented enabled the identification of new nitrogen- and metal-containing ions. For the metal-containing ions, their relative ion abundances were below 0.03% in all cases. From all metal-containing ions, the highest contribution was from the $[Fe(OH)_2]H^+$ ion in the PTR-3 and in PTR-1 with relative ion abundances of 0.002% and 0.003%, respectively. For the PTR-2, the Fe^+ ion appeared as dominant (0.023%), followed by the $[Fe(OH)_2]H^+$ ion (0.006%). These ions could be used as aging indicators of the ion source. The assignment of a memory effect as such appeared to be a challenging task, since a substance that is present as memory effect can simultaneously be present as impurity in the inert purging gas. Based on the gathered information, a database of trace compounds in PTR instruments with their respective origins is built up, which may help PTR users to elucidate artefacts and differentiate them from real VOCs, especially in cases where dilution with inert gases plays a crucial role, thus preventing misinterpretations

and wrong estimations. This database can be found under www.cec.mpg.de, and it will be updated regularly with new findings.

CONFLICT OF INTEREST

The authors declare no conflict of interest.

ORCID

Jorge Iván Salazar Gómez https://orcid.org/0000-0002-6274-9530

REFERENCES

1. Munson MSB, Field FH. Chemical ionization mass spectrometry. I. General introduction. *J Am Chem Soc*. 1966;88:2621-2630.

2. Munson B. CIMS, Chemistry in mass spectrometry. *Int J Mass Spectrom*. 2015;377:502-506.

3. Lindinger W, Hansel A, Jordan A. Proton-transfer-reaction mass spectrometry (PTR–MS): on-line monitoring of volatile organic compounds at pptv levels. *Chem Soc Rev*. 1998;27:347–354.

4. Hansel A, Jordan A, Holzinger R, Prazeller P, Vogel W, Lindinger W. Proton transfer reaction mass spectrometry: on-line trace gas analysis at the ppb level. *Int J Mass Spectrom Ion Processes*. 1995;149-150:609-619.

5. Yeretzian C, Jordan A, Lindinger W. Analysing the headspace of coffee by proton-transfer-reaction mass-spectrometry. *Int J Mass Spectrom*. 2003;223-224:115-139.

6. Romano A, Fischer L, Herbig J, et al. Wine analysis by FastGC proton-transfer reaction-time-of-flight-mass spectrometry. *Int J Mass Spectrom*. 2014;369:81-86.

7. Masi E, Romani A, Pandolfi C, Heimler D, Mancuso S. PTR-TOF-MS analysis of volatile compounds in olive fruits. *J Sci Food Agric*. 2015;95(7):1428-1434.

8. Lagg A, Taucher J, Hansel A, Lindinger W. Applications of proton transfer reactions to gas analysis. *Int J Mass Spectrom Ion Processes*. 1994;134:55-66.

9. Lindinger W, Hansel A, Jordan A. On-line monitoring of volatile organic compounds at pptv levels by means of proton-transfer-reaction mass spectrometry (PTR-MS) medical applications, food control and environmental research. *Int J Mass Spectrom Ion Processes*. 1998;173:191-241.

10. Hayward S, Hewitt CN, Sartin JH, Owen SM. Performance characteristics and applications of a proton transfer reaction-mass spectrometer for measuring volatile organic compounds in ambient air. *Environ Sci Technol*. 2002;36(7):1554-1560.

11. D'Anna B, Wisthaler A, Andreasen O, et al. Atmospheric chemistry of C3-C6 cycloalkanecarbaldehydes. *J Phys Chem A*. 2005;109(23):5104-5118.

12. de Gouw J, Warneke C. Measurements of volatile organic compounds in the earth's atmosphere using proton-transfer-reaction mass spectrometry. *Mass Spectrom Rev*. 2007;26(2):223-257.

13. Biasioli F, Gasperi F, Odorizzi G, et al. PTR-MS monitoring of odour emissions from composting plants. *Int J Mass Spectrom*. 2004;239:103-109.

14. Clementschitsch F, Bayer K. Improvement of bioprocess monitoring: development of novel concepts. *Microb Cell Fact*. 2006;5:19.

15. Morken AK, Nenseter B, Pedersen S, et al. Emission results of amine plant operations from MEA testing at the CO2 Technology Centre Mongstad. *12th Int Conf Greenhouse Gas Contr Technol, Ghgt-12*. 2014;63:6023-6038.

16. Sanchez-Lopez JA, Zimmermann R, Yeretzian C. Insight into the time-resolved extraction of aroma compounds during espresso coffee preparation: online monitoring by PTR-ToF-MS. *Anal Chem*. 2014;86(23):11696-11704.

17. Herbig J, Gutmann R, Winkler K, Hansel A, Sprachmann G. Real-time monitoring of trace gas concentrations in syngas. *Oil Gas Sci Technol – Rev IFP Energies nouvelles*. 2013;69:363-372.

18. Agarwal B, Jurschik S, Sulzer P, et al. Detection of isocyanates and polychlorinated biphenyls using proton transfer reaction mass spectrometry. *Rapid Commun Mass Spectrom*. 2012;26:983-989.

19. Bukhtiyarov VI, Nizovskii AI, Bluhm H, et al. Combined in situ XPS and PTRMS study of ethylene epoxidation over silver. *J Catal*. 2006;238:260-269.

20. Španěl P, Smith D. SIFT studies of the reactions of H_3O^+, NO^+ and O_2^+ with a series of alcohols. *Int J Mass Spectrom Ion Processes*. 1997;167-168:375-388.

21. Tani A, Hayward S, Hewitt CN. Measurement of monoterpenes and related compounds by proton transfer reaction-mass spectrometry (PTR-MS). *Int J Mass Spectrom*. 2003;223-224:561-578.

22. Graus M, Müller M, Hansel A. High resolution PTR-TOF: quantification and formula confirmation of VOC in real time. *J Am Soc Mass Spectrom*. 2010;21(6):1037-1044.

23. Blake RS, Whyte C, Hughes CO, Ellis AM, Monks PS. Demonstration of proton-transfer reaction time-of-flight mass spectrometry for real-time analysis of trace volatile organic compounds. *Anal Chem*. 2004;76:3841-3845.

24. Pang X. Biogenic volatile organic compound analyses by PTR-TOF-MS: calibration, humidity effect and reduced electric field dependency. *J Environ Sci (China)*. 2015;32:196-206.

25. Brown P, Watts P, Märk TD, Mayhew CA. Proton transfer reaction mass spectrometry investigations on the effects of reduced electric field and reagent ion internal energy on product ion branching ratios for a series of saturated alcohols. *Int J Mass Spectrom*. 2010;294:103-111.

26. Romano A, Hanna GB. Identification and quantification of VOCs by proton transfer reaction time of flight mass spectrometry: an experimental workflow for the optimization of specificity, sensitivity, and accuracy. *J Mass Spectrom*. 2018;53(4):287-295.

27. de Gouw JA, Goldan PD, Warneke C, et al. Validation of proton transfer reaction-mass spectrometry (PTR-MS) measurements of gas-phase organic compounds in the atmosphere during the New England Air Quality Study (NEAQS) in 2002. *J Geophys Res: Atmospheres*. 2003;108:4682.

28. Yuan B, Koss A, Warneke C, et al. A high-resolution time-of-flight chemical ionization mass spectrometer utilizing hydronium ions (H3O + ToF-CIMS) for measurements of volatile organic compounds in the atmosphere *Atmos. Meas Tech*. 2016;9:2735-2752.

29. Bukhtiyarova M, Lunkenbein T, Kähler K, Schlögl R. Methanol synthesis from industrial CO_2 sources: a contribution to chemical energy conversion. *Catal Lett*. 2017;147:416-427.

30. Thornberry T, Murphy DM, Thomson DS, et al. Measurement of aerosol organic compounds using a novel collection/thermal-desorption PTR-ITMS instrument. *Aerosol Sci Tech*. 2009;43:486-501.

31. Crespo E, Devasena S, Sikkens C, Centeno R, Cristescu SM, Harren FJ. Proton-transfer reaction mass spectrometry (PTRMS) in combination with thermal desorption (TD) for sensitive off-line analysis of volatiles. *Rapid Commun Mass Spectrom*. 2012;26:990-996.

32. Sulzer P, Hartungen E, Hanel G, et al. A proton transfer reaction-quadrupole interface time-of-flight mass spectrometer (PTR-QiTOF): high speed due to extreme sensitivity. *Int J Mass Spectrom*. 2014; 368:1-5.

33. Smith D, Adams NG, Miller TM. A laboratory study of the reactions of N^+, N_2^+, N_3^+, N_4^+, O^+, O_2^+, and NO^+ ions with several molecules at 300 K. *J Chem Phys*. 1978;69:308–318.

34. Bierbaum VM, Kaufman F. Kinetics of the reactions of N_2H^+, N_4^+, and N_3^+ with H2O in the gas phase. *J Chem Phys*. 1974;61:3804-3809.

35. Fehsenfeld FC, Schmeltekopf AL, Ferguson EE. Thermal-energy ion—neutral reaction rates. VII. Some hydrogen-atom abstraction reactions. *J Chem Phys*. 1967;46:2802-2808.

36. Howorka F, Lindinger W, Varney RN. Reaction-rate constants in steady-state hollow-cathode discharges: $N_2 + H_2O$ Reactions. *J Chem Phys*. 1974;61:1180-1188.

37. Milligan DB, Wilson PF, Freeman CG, Meot-Ner M, McEwan MJ. Dissociative proton transfer reactions of H_3^+, N_2H^+, and H_3O^+ with acyclic, cyclic, and aromatic hydrocarbons and nitrogen compounds, and astrochemical implications. *J Phys Chem A*. 2002;106:9745-9755.

38. Warneke C, de Gouw JA, Kuster WC, Goldan PD. Validation of atmospheric VOC measurements by proton-transfer-reaction mass spectrometry using a gas-chromatographic preseparation method R. Fall. *Environ Sci Technol*. 2003;37:2494-2501.

39. Müller M, Mikoviny T, Feil S, et al. A compact PTR-ToF-MS instrument for airborne measurements of volatile organic compounds at high spatiotemporal resolution. *Atmos Meas Tech*. 2014;7:3763-3772.

40. Norman M, Hansel A, Wisthaler A. O_2^+ as reagent ion in the PTR-MS instrument: detection of gas-phase ammonia. *Int J Mass Spectrom*. 2007;265:382-387.

41. Lin CS, Liou NW, Chang PE, Yang JC, Sun E. Fugitive coke oven gas emission profile by continuous line averaged open-path Fourier transform infrared monitoring. *J Air Waste Manage Assoc*. 2007;57(4): 472-479.

42. Ekgauz VI, Pokryshkin KV, Tretiakova GD, et al. Removal of ammonia from coke-oven gas at PAO Severstal' by a circulatory phosphate method. *Coke Chem*. 2016;59:92-100.

43. Awe OW, Zhao YQ, Nzihou A, Minh DP, Lyczko N. A review of biogas utilisation, purification and upgrading technologies. *Waste Biomass Valor*. 2017;8:267-283.

44. Adams NG, Smith D, Paulson JF. An experimental survey of the reactions of NH_n^+ ions (n = 0 to 4) with several diatomic and polyatomic molecules at 300 K. *J Chem Phys*. 1980;72:288-297.

45. Albritton DL, Dotan I, Lindinger W, McFarland M, Tellinghuisen J, Fehsenfeld FC. Effects of ion speed distributions in flow-drift tube studies of ion–neutral reactions. *J Chem Phys*. 1977;66:410-421.

46. McFarland M, Albritton DL, Fehsenfeld FC, Ferguson EE, Schmeltekopf AL. Flow-drift technique for ion mobility and ion-molecule reaction rate constant measurements. II. Positive ion reactions of N^+, O^+, and H_2^+ with O_2 and O^+ with N_2 from thermal to ~2 eV. *J Chem Phys*. 1973;59:6620-6628.

47. Müller M, Graus M, Ruuskanen TM, et al. First eddy covariance flux measurements by PTR-TOF. *Atmos Meas Tech*. 2010;3(2):387-395.

48. Millar TJ, Farquhar PRA, Willacy K. The UMIST database for astrochemistry 1995. *Astron Astrophys Suppl Ser*. 1997;121:139-185.

49. Le Teuff YH, Millar TJ, Markwick AJ. The UMIST database for astrochemistry 1999. *Astron Astrophys Suppl Ser*. 2000;146:157-168.

50. Jobson BT, McCoskey JK. Sample drying to improve HCHO measurements by PTR-MS instruments: laboratory and field measurements. *Atmos Chem Phys*. 2010;10:1821-1835.

51. Hansel A, Singer W, Wisthaler A, Schwarzmann M, Lindinger W. Energy dependencies of the proton transfer reactions $H_3O(+)+CH_2O$ double left right arrow CH_2OH++H_2O. *Int J Mass Spectrom*. 1997;167:697-703.

52. Inomata S, Tanimoto H, Kameyama S, et al. Technical note: determination of formaldehyde mixing ratios in air with PTR-MS: laboratory experiments and field measurements. *Atmos Chem Phys*. 2008;8: 273-284.

53. Vlasenko A, Macdonald AM, Sjostedt SJ, Abbatt JPD. Formaldehyde measurements by Proton transfer reaction – Mass Spectrometry (PTR-MS): correction for humidity effects. *Atmos Meas Tech*. 2010;3:1055-1062.

54. Jankowski MJ, Olsen R, Nielsen CJ, Thomassen Y, Molander P. The applicability of proton transfer reaction-mass spectrometry (PTR-MS) for determination of isocyanic acid (ICA) in work room atmospheres. *Environ Sci: Processes Impacts*. 2014;16(10):2423-2431.

55. Pavageau M-P, Pécheyran C, Krupp EM, Morin A, Donard OFX. Volatile metal species in coal combustion flue gas. *Environ Sci Technol*. 2002;36(7):1561-1573.